

ISSN: 1672 - 6553

**JOURNAL DYNAMICS
AND CONTROL**

VOLUME 10 ISSUE 05: P177-184

A COMPARATIVE INVESTIGATION
OF POWER CONVERSION
CAPABILITY IN SISO AND MISO DC-
DC BOOST CONVERTER
CONFIGURATIONS

Monika Meena¹, Tarun Naruka²

¹PG Scholar, ²Associate Professor
Swami Keshvanand Institute of technology
Management & Gramothan,
Jaipur – 302017, India

A COMPARATIVE INVESTIGATION OF POWER CONVERSION CAPABILITY IN SISO AND MISO DC–DC BOOST CONVERTER CONFIGURATIONS

Monika Jagat Meena¹, Tarun Naruka²

¹PG Scholar, ²Associate Professor

Swami Keshvanand Institute of technology Management & Gramothan,
Jaipur – 302017, India

minamonikajagat@gmail.com, tarun.naruka@skit.ac.ins

Received on: 5th March, 2026; Revised on: 25th, May, 2026; Published on 5th June, 2026

Abstract- DC–DC boost converters are widely used in modern power electronic systems to step up low input voltage to a higher regulated output. This paper presents a comparative analysis of Single Input Single Output (SISO) and Multi-Input Single Output (MISO) boost converter topologies. The SISO converter, based on inductor energy storage and controlled switching, is simple, cost-effective, and suitable for low-power applications. This work presents a unified comparative investigation of SISO and MISO boost converters under multiple operating conditions using small-signal state-space modeling and MATLAB/Simulink analysis. The proposed study additionally evaluates the dynamic behavior and stability characteristics of hybrid-source MISO configurations incorporating DC, AC, and fuel-cell inputs, thereby providing practical insight for renewable-energy-based power conversion systems.

Keywords–DC-DC Boost Converter, SISO Converter, MISO Converter, Hybrid Energy System, Small Signal Modeling, Renewable Energy Integration.

1. INTRODUCTION

The increasing demand for efficient energy utilization and advanced power management systems has led to significant developments in DC–DC converter technologies. Among these, boost converters are widely used due to their ability to step up a low input voltage to a higher, regulated output voltage, making them essential in applications such as renewable energy systems, electric vehicles, battery-powered devices, and portable electronics.[1],[3],[21]

The Single Input Single Output (SISO) boost converter is one of the most fundamental and commonly used topologies in power electronics. Its simple design, ease of control, and cost-effectiveness make it highly suitable for applications where only a single energy source is available. The SISO converter operates on the principle of storing energy in an inductor during the switching ON state and releasing it to the load during the OFF state, thereby achieving voltage amplification with relatively high efficiency.[5],[24]

However, with the growing adoption of hybrid energy systems that combine multiple sources such as solar panels, batteries, and fuel cells, the limitations of single-input converters have become evident. This has led to the development of Multi-Input Single Output (MISO) boost converters, which are capable of integrating multiple energy sources into a unified system. MISO converters offer enhanced flexibility, improved reliability, and better energy utilization by allowing simultaneous or independent operation of different input sources.[11],[12],[13]

The objective of this study is to assist in selecting the most appropriate converter topology for specific applications, particularly in modern energy systems where efficiency, reliability, and sustainability are of paramount importance. Most existing research primarily focuses either on conventional SISO boost converters or on isolated studies of multi-input converter topologies. Limited work has been reported on the comparative dynamic analysis of SISO and MISO boost converters under hybrid energy operating conditions using unified small-signal modeling techniques. In this work, a comprehensive comparison between SISO and MISO converter configurations is presented considering voltage gain, ripple behavior, efficiency, and stability performance. Furthermore, the proposed MISO system is investigated under different source combinations including DC–DC, DC–AC, and fuel-cell-based hybrid configurations to evaluate converter suitability for renewable energy applications.

Here we use the following algorithm to analysis boost converter topologies:[23],[27]

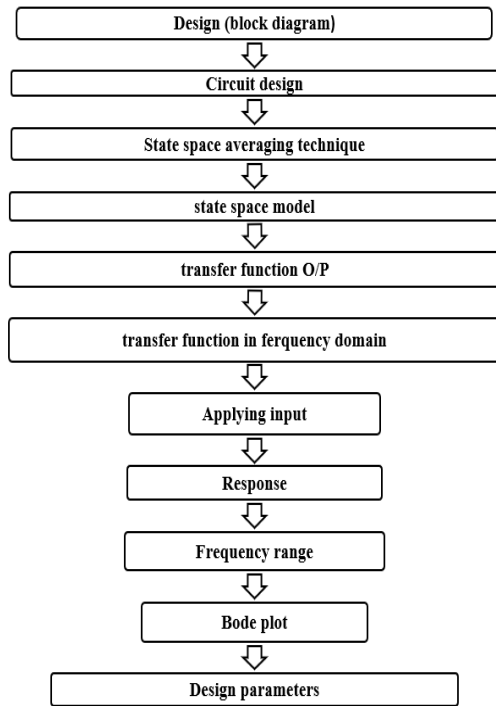


Figure 1: Algorithm

2. SINGLE INPUT-SINGLE OUTPUT (SISO)

Boost converters are a type of DC-DC switching converter that efficiently increase (step-up) the input voltage to a higher output voltage. By storing energy in an inductor during the switch-on phase and releasing it to the load during the switch-off phase, this voltage conversion is made possible. Power electronics applications requiring a greater output voltage than the input source, in particular, depend on boost converters.[6],[7]

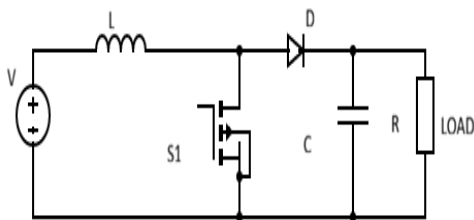


Figure 2: Typical boost converter circuit diagram

Components:

- Input voltage: V_{in}
- Inductor: L
- Switch (MOSFET)
- Diode: D

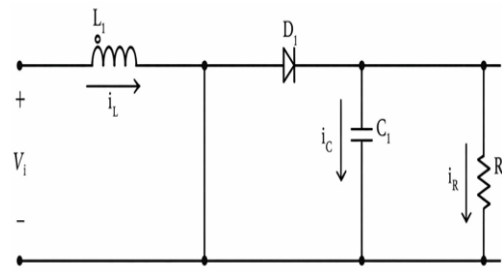
- Output capacitor: C
- Load resistor: R

Control variable: Duty ratio D of the switch.

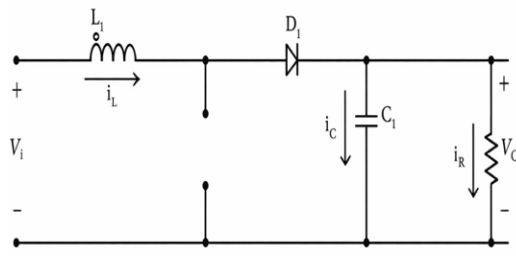
We analyze in **Continuous Conduction Mode (CCM)**. [1],[4]

2.1 operating principle of boost converter:

The basic operating principle of a boost converter can be understood through the following two stages:



(a)



(b)

Figure 3: (a) boost converter ON state, (b) boost converter OFF state

2.1.1 Switch ON (for duration DT):

During this stage, the input voltage (V_{in}) is applied across the inductor (L), causing the current through the inductor to increase linearly. The energy stored in the inductor builds up, and the diode (D) is reverse-biased, preventing current flow to the load.

$$V_L = V_{in}$$

i_L increases ,

$$\frac{di_L}{dt} = \frac{V_{in}}{L}$$

$$i_c = -\frac{v_o}{R} \text{ (load current through capacitor)}$$

2.1.2 Switch OFF for duration (1-D)T:

When the switch S1 opens, the inductor current must continue to flow. This forces the diode D to become forward-biased, and the inductor releases its stored energy to the load (R) and the output capacitor (C). During this period, the voltage across the inductor (V_L) is equal to the difference between the output voltage (V_{out}) and the input voltage (V_{in}). The inductor current decreases linearly as the energy is transferred to the load.

$$V_L = V_{in} - v_o$$

$$i_L \text{ decreases, } \frac{di_L}{dt} = \frac{V_{in} - v_o}{L}$$

$$i_c = i_L - \frac{v_o}{R}$$

2.2 transfer function for boost converter (small signal CCM):

State-space equation for both intervals:

Let the states be:

$$x_1 = i_L, x_2 = v_o$$

(a) switch ON

$$[i_L \ v_o] = \begin{bmatrix} 0 & 0 & 0 & -\frac{1}{RC} \end{bmatrix} [i_L \ v_o] + \begin{bmatrix} \frac{1}{L} & 0 \end{bmatrix} V_{in}$$

(b) switch OFF

$$[i_L \ v_o] = \begin{bmatrix} 0 & -\frac{1}{L} & \frac{1}{C} & -\frac{1}{RC} \end{bmatrix} [i_L \ v_o] + \begin{bmatrix} \frac{1}{L} & 0 \end{bmatrix} V_{in}$$

Averaged state-space model: [2],[4],[9],[10]

In steady state, average the two modes according to the duty ratio D:

$$\dot{x} = Ax + BV_{in}$$

Where, $A = DA_{on} + (1-D)A_{off}$,

$$B = DB_{on} + (1-D)B_{off}$$

Substitutes matrices:

$$A = \begin{bmatrix} 0 & \frac{-(1-D)}{L} & \frac{(1-D)}{C} & \frac{-1}{RC} \end{bmatrix},$$

$$B = \begin{bmatrix} \frac{1}{L} & 0 \end{bmatrix}$$

So average model becomes:

$$\begin{bmatrix} \dot{i}_L & \dot{v}_o \end{bmatrix} = \begin{bmatrix} 0 & -\frac{(1-D)}{L} & \frac{(1-D)}{C} & -\frac{1}{RC} \end{bmatrix} \begin{bmatrix} i_L & v_o \end{bmatrix} + \begin{bmatrix} \frac{1}{L} & 0 \end{bmatrix} V_{in} \quad (1)$$

Steady state relations:

At steady-state ($\dot{i}_L = 0, \dot{v}_o = 0$):

From inductor equation (1st row):

$$0 = -\frac{(1-D)}{L} V_o + \frac{1}{L} V_{in} \rightarrow V_o = \frac{V_{in}}{(1-D)} \quad (2)$$

From capacitor equation (2nd row)

$$0 = \frac{(1-D)}{C} I_L - \frac{V_o}{RC} \rightarrow I_L = \frac{V_o}{R(1-D)} \quad (3)$$

Introduce small perturbation:

$$D = D + \hat{d}, i_L = I_L + \hat{i}_L, v_o = V_o + \hat{v}_o$$

Linearize equation(1) around the steady-state.

Substitute and linearize:

For the inductor:

$$L \frac{d(\hat{i}_L)}{dt} = V_{in} - (1-D)v_o$$

$$L \frac{d(\hat{i}_L)}{dt} = -(1-D)\hat{v}_o + V_o \hat{d} \quad (4)$$

For the capacitor:

$$C \frac{d(\hat{v}_o)}{dt} = (1-D)\hat{i}_L - \frac{v_o}{R}$$

Linearizing gives:

$$C \frac{d(\hat{v}_o)}{dt} = (1-D)\hat{i}_L - I_L \hat{d} - \frac{\hat{v}_o}{R} \quad (5)$$

Convert to Laplace(frequency) domain:

$$Ls\hat{i}_L = -(1-D)\hat{v}_o + V_o \hat{d} \quad (6)$$

$$Cs\hat{v}_o = (1-D)\hat{i}_L - I_L \hat{d} - \frac{\hat{v}_o}{R} \quad (7)$$

Substitute (6) into (7)

From(6):

$$\hat{i}_L = \frac{(1-D)\hat{v}_o + V_o \hat{d}}{Ls}$$

Substitute in(7)

$$Cs\hat{v}_o = (1-D) \frac{-(1-D)\hat{v}_o + V_o \hat{d}}{Ls} - I_L \hat{d} - \frac{\hat{v}_o}{R}$$

Simplify terms:

$$Cs\hat{v}_o = -\frac{(1-D)^2}{Ls} \hat{v}_o + \frac{(1-D)V_o \hat{d}}{Ls} - I_L \hat{d} - \frac{\hat{v}_o}{R}$$

By collecting terms:

Multiply through by Ls

$$LCs^2\hat{v}_o + \frac{L}{R}s\hat{v}_o + (1-D)^2 = [(1-D)V_o - LsI_L]\hat{d}$$

Transfer function:

$$G_{vd}(s) = \frac{\hat{v}_o(s)}{\hat{d}(s)} = \frac{(1-D)V_o - LsI_L}{LCs^2 + \frac{Ls}{R} + (1-D)^2} \quad (8)$$

This is the boost converter small-signal duty-to-output transfer function.[1],[2],[9]

Substitute steady-state relationships (2) and (3)

$$V_o = \frac{V_{in}}{(1-D)} \quad , I_L = \frac{V_{in}}{R(1-D)^2}$$

Substitute into (8):

$$G_{vd} = \frac{V_{in}(1 - \frac{Ls}{R(1-D)^2})}{LCs^2 + \frac{Ls}{R} + (1-D)^2} \quad (9)$$

In frequency domain: putting $s \rightarrow j\omega$ in equation(9)

$$G_{vd}(j\omega) = \frac{V_{in}(1 - j\frac{\omega L}{R(1-D)^2})}{-LC\omega^2 + j\frac{L}{R}\omega + (1-D)^2}$$

2.3 Case study:

We analyze the SISO converter using the following parameters.:

- $V_{in}=12$ volt
- $L= 13.92 \mu\text{H}$
- $C=27.5 \mu\text{F}$
- $R=20\Omega$
- $f=10\text{kHz}$
- Duty cycle = 0.5

Table 1: Case study for SISO converter

Input	Transfer function
Impulse input $s \rightarrow 1$	$\frac{48 - 1.33632 \times 10^{-4}s}{1.5312 \times 10^{-9}s^2 + 2.784 \times 10^{-6}s + 1}$
Step input $s \rightarrow \frac{1}{s}$	$\frac{576 - 0.001603584s}{1.5312 \times 10^{-9}s^3 + 2.784 \times 10^{-6}s^2 + s}$
Ramp input $s \rightarrow \frac{1}{s^2}$	$\frac{576 - 0.001603584s}{1.5312 \times 10^{-9}s^4 + 2.784 \times 10^{-6}s^3 + s^2}$

Arbitrary input $s \rightarrow \frac{1}{s+1}$	$\frac{48 - 1.33632 \times 10^{-4}s}{1.5312 \times 10^{-9}s^3 + 2.7855 \times 10^{-6}s^2 + 1.000002784s + 1}$
---	---

3. MULTI INPUT-SINGLE OUTPUT (MISO)

MISO converter accepts multiple DC inputs (PV, battery, fuel cell, supercapacitor, etc.) and produces one controlled output voltage.[8],[16],[26]

MISO used for

- Hybrid energy systems[21],[22]
- Renewable + storage integration[29]
- Reduced component count
- Independent power sharing
- Higher reliability

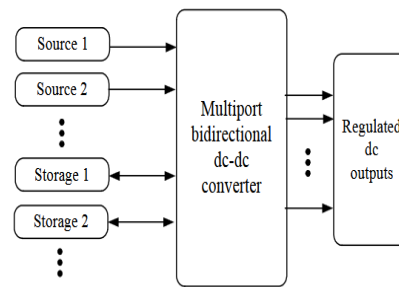


Figure 4: Multiport system structure

A multi-input single-output (MISO) boost converter enables effective integration of multiple energy sources into a common DC bus while ensuring regulated output voltage and controllable power sharing among sources.[14],[15],[17]

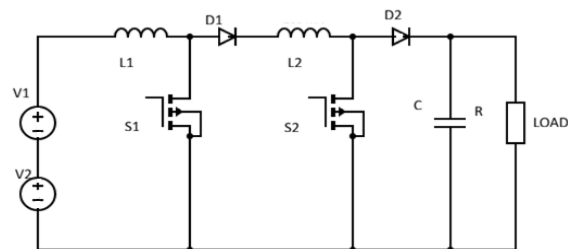


Figure 5: Two input-single output boost converters

3.1 Operating principle:

3.1.1 Mode-I : Switches ON State

When switches S_1 and S_2 are turned ON:

- Inductors L_1 and L_2 are directly connected to their input sources.
- Current through inductors starts increasing linearly. [18]

- Energy is stored in magnetic form inside the inductors.
- Diodes D_1 and D_2 become reverse biased.
- Load receives power from the output capacitor.[19]

3.1.2 Mode-II : Switches OFF State

- When switches S_1 and S_2 are turned OFF:
- Inductor current cannot change instantly.
- Polarity across inductors reverses.
- Diodes become forward biased.
- Stored energy transfers to:
 - Output capacitor
 - Load resistor

Now both input sources and inductors together supply the load.

3.2 Transfer function for proposed MISO converter: [25]

State variables:

$$x_1 = i_{L1}, x_2 = i_{L2}, x_3 = V_o$$

On state (switches on)

Inductor charge from sources:

$$\frac{di_{L1}}{dt} = \frac{V_1}{L_1}, \quad (1)$$

$$\frac{di_{L2}}{dt} = \frac{V_2}{L_2}, \quad (2)$$

Capacitor supplies load:

$$\frac{dV_o}{dt} = -\frac{V_o}{RC} \quad (3)$$

OFF state (switches off)

Inductor discharges to output:

$$\frac{di_{L1}}{dt} = \frac{V_1 - V_o}{L_1},$$

$$\frac{di_{L2}}{dt} = \frac{V_2 - V_o}{L_2},$$

$$\frac{dV_o}{dt} = \frac{i_{L1} + i_{L2}}{C} - \frac{V_o}{RC} \quad (4)$$

Averaged state-space model:[2],[4],[9],[10]

Inductor L1:

$$\begin{aligned} \frac{di_{L1}}{dt} &= D \frac{V_1}{L_1} + (1 - D) \frac{V_1 - V_o}{L_1}, \\ &= \frac{V_1}{L_1} - (1 - D) \frac{V_o}{L_1} \end{aligned} \quad (5)$$

Inductor L2:

$$\frac{di_{L2}}{dt} = \frac{V_2}{L_2} - (1 - D) \frac{V_o}{L_2}, \quad (6)$$

Output capacitor:

$$\frac{dV_o}{dt} = (1 - D) \frac{i_{L1} + i_{L2}}{C} - \frac{V_o}{RC} \quad (7)$$

Steady state voltage gain:

At steady state:

$$\frac{di}{dt} = 0$$

$$\text{So, } V_o = \frac{V_1 + V_2}{1 - D} \quad (8)$$

Small signal linearization:

$$\text{Perturbation: } D = D + \hat{d}, V_o = V_o + \hat{v}_o$$

Linearize capacitor equation (control \rightarrow output)

$$\frac{d\hat{v}_o}{dt} = \frac{(1 - D)}{C} (\hat{i}_{L1} + \hat{i}_{L2}) - \frac{\hat{v}_o}{RC} - \frac{(i_{L1} + i_{L2})}{C} \hat{d}$$

Control-to-output transfer function:

$$G(s) = \frac{\widehat{V}_o(s)}{\widehat{D}(s)}$$

Final form:

$$G(s) = \frac{V_o}{1 - D} \cdot \frac{1 - s \frac{L_{eq}}{R(1 - D)^2}}{L_{eq} C s^2 + \frac{L_{eq}}{R} s + (1 - D)^2} \quad (9)$$

Where equivalent inductance:

$$L_{eq} = \frac{L_1 L_2}{L_1 + L_2}$$

3.3 case study

The MISO converter was simulated using the following parameters:

$$V1_{input} = 12\text{v}$$

$$V2_{input} = 24\text{v}$$

$$L_1, L_2 = 50\text{e-}6 \text{ H}$$

$$C = 700\text{e-}6 \text{ F}$$

$$R = 300 \Omega$$

$$f = 20 \text{ kHz}$$

$$D = 0.5$$

Table 2: case study of MISO converter

Case No.	Input 1	Input 2
Case 1	12V	24vV
Case 2	12V	Ac source
Case 3	12V	Fuel cell 24v

4. SIMULATION AND RESULTS

4.1 Stability analysis for different inputs of SISO converter:

Using a variety of standard excitation signals such as impulse, step, ramp and arbitrary inputs, performance of the SISO system was evaluated with MATLAB Tool.[1],[5],[20]

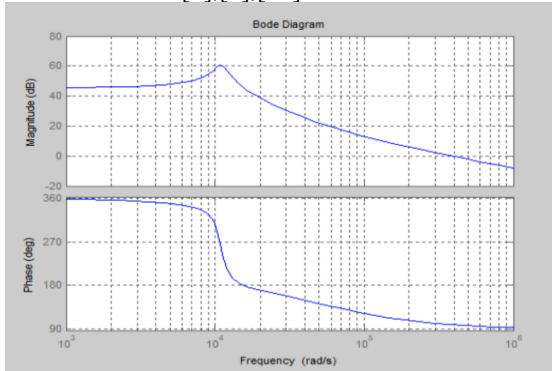


Figure 6: Output for impulse input

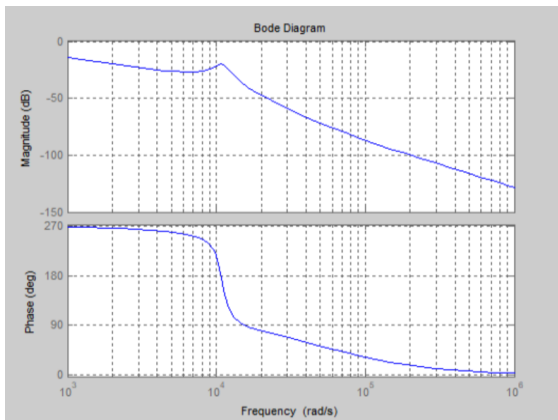


Figure 7: Output for step input

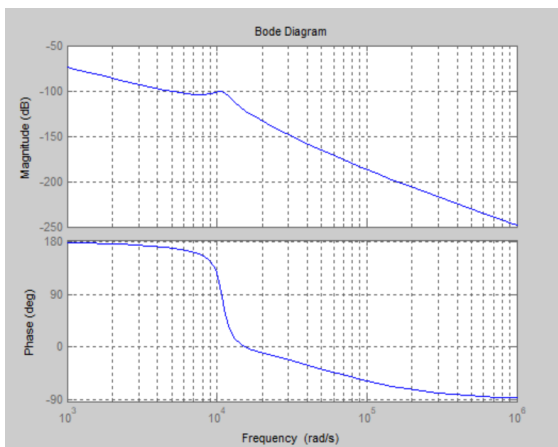


Figure 8: output for ramp input

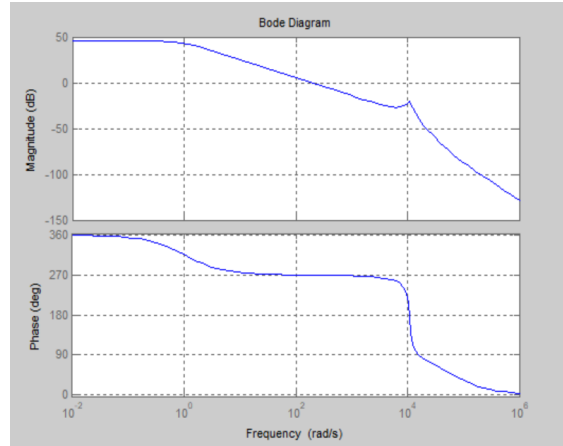


Figure 9: Output for arbitrary input

4.2 Responses for MISO converter in deferent cases as per table no. 2

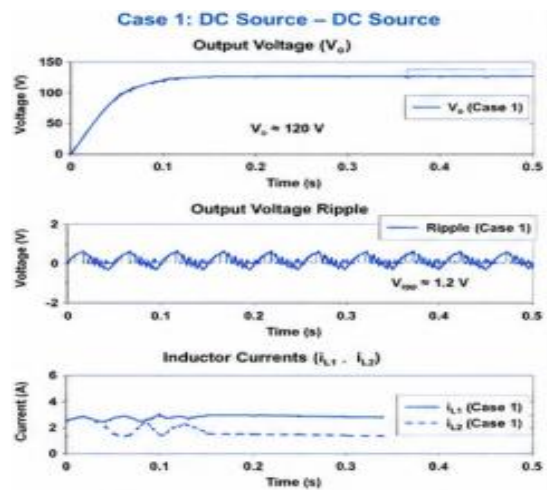


Figure 10: Response of the MISO boost converter in case 1

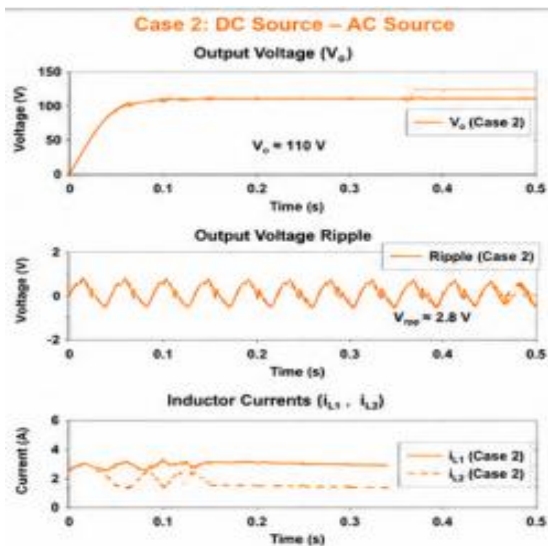


Figure 11: Response of the MISO converter in case 2

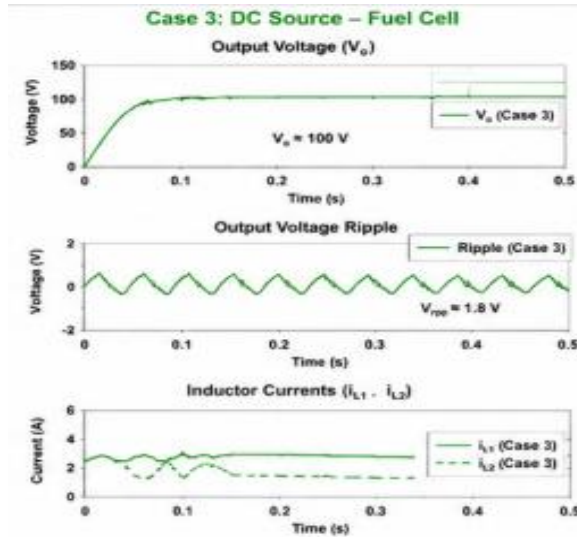


Figure 12: Response of the MISO boost converter for case

The MISO converter was analyzed under different case study as per the table no 2. The first case is when both the inputs are 12V DC, under this highest output achieved with highest efficiency among all three cases as shown in figure 10. Bode plot analysis further validated the converter’s stability by demonstrating sufficient gain and phase margins. In Case 2 when one of the input is 12V and other one is AC source then, first AC source is rectified as per the requirement, but in this case the response is moderate and AC source introduces more ripple as highlighted in the figure 11. In figure 12 the case 3 response is highlighted, in which the fuel-cell-based configuration demonstrated a lower crossover frequency because fuel cells inherently possess slower dynamic response characteristics compared to other energy sources.

Table 3: Performance summary for MISO boost converter

Performance Summary				
Parameter	Case 1 (DC-DC)	Case 2 (DC-AC)	Case 3 (DC-Fuel Cell)	Conclusion/Fact
Steady State Output (V_o)	≈ 120 V	≈ 110 V	≈ 100 V	Highest output in Case 1
Voltage Ripple (V_{rpp})	≈ 1.2 V	≈ 2.8 V	≈ 1.8 V	AC source introduces more ripple
Efficiency (η)	≈ 92.5 %	≈ 87.0 %	≈ 89.0 %	Case 1 has highest efficiency
Inductor Current(Avg)	≈ 2.6 A / 2.3 A	≈ 2.9 A / 2.5 A	≈ 2.4 A / 2.1 A	Current stress moderate in Case 3
Stability	High	Moderate	Good	AC source causes more variability
Suitability	Best for stable DC systems	Good for hybrid AC systems	Good for renewable systems	Choose based on application

5. CONCLUSION

The major contribution of this work lies in the unified comparative evaluation of SISO and MISO boost converter configurations through small-signal modeling and stability analysis under multiple hybrid-source operating conditions. The presented analysis provides useful design insight for future renewable-energy-based power electronic systems requiring flexible multi-source integration and stable voltage regulation.

Small-signal analysis of the proposed MISO boost converter was performed to investigate the dynamic behavior and stability of the system under small variations in input voltage and duty cycle. The nonlinear converter model was linearized around the steady-state operating point using state-space averaging techniques. The derived transfer function establishes the relationship between duty cycle and output voltage, which is essential for controller

design. Results indicate stable operation for all investigated cases under continuous conduction mode (CCM). Among the considered configurations, the DC–DC case exhibited the fastest dynamic response, lower overshoot, and better settling characteristics. Bode plot analysis further confirmed the stability of the converter through adequate gain and phase margins. The DC–AC case showed reduced phase margin due to harmonic distortion, while the fuel-cell-based configuration exhibited lower crossover frequency because of slower source dynamics. Overall, the proposed converter demonstrated stable and reliable performance for hybrid energy applications.

REFERENCES

- [1] Fundamentals of Power Electronics, R. W. Erickson and D. Maksimović, *Fundamentals of Power Electronics*, 2nd ed., Springer, Boston, 2001.

- [2] R. D. Middlebrook and S. Čuk, "A General Unified Approach to Modelling Switching-Converter Power Stages," *IEEE Power Electronics Specialists Conference (PESC)*, pp. 18–34, 1976.
- [3] N. Mohan, T. M. Undeland, and W. P. Robbins, *Power Electronics: Converters, Applications, and Design*, 3rd ed., John Wiley & Sons, 2003.
- [4] D. Maksimović and S. Čuk, "Switching Converters with Wide DC Conversion Range," *IEEE Transactions on Power Electronics*, vol. 6, no. 1, pp. 151–157, Jan. 1991.
- [5] M. H. Rashid, *Power Electronics: Circuits, Devices and Applications*, 4th ed., Pearson Education, 2014.
- [6] R.D. Middlebrook, "A continuous model for the tapped-inductor boost converter," *IEEE power electronics specialists conference*, 1975 record, pp.63-79 (IEEE publication 75 CHO 965-4-AES)
- [7] Y. P. Hsieh, J. F. Chen, T. J. Liang, and L. S. Yang, "Novel High Step-Up DC–DC Converter for Distributed Generation System," *IEEE Transactions on Industrial Electronics*, vol. 60, no. 4, pp. 1473–1482, Apr. 2013.
- [8] S. K. Changchien, T. J. Liang, J. F. Chen, and L. S. Yang, "Novel High Step-Up DC–DC Converter for Fuel Cell Energy Conversion System," *IEEE Transactions on Industrial Electronics*, vol. 57, no. 6, pp. 2007–2017, June 2010.
- [9] V. Vorperian, "Simplified Analysis of PWM Converters Using Model of PWM Switch," *IEEE Transactions on Aerospace and Electronic Systems*, vol. 26, no. 3, pp. 490–496, May 1990.
- [10] J. Sun, D. M. Mitchell, M. F. Greuel, P. T. Krein, and R. M. Bass, "Averaged Modeling of PWM Converters Operating in Discontinuous Conduction Mode," *IEEE Transactions on Power Electronics*, vol. 16, no. 4, pp. 482–492, July 2001.
- [11] M. Marchesoni and C. Vacca, "New DC-DC converter for energy storage system interfacing in fuel cell hybrid electric vehicles," *IEEE Trans. Power Electron.*, vol. 22, no. 1, pp. 301–308, Jan. 2007.
- [12] B. Wang, L. Xian, X. Zhang, and H. B. Gooi, "A MPC-Based Method for Single-Inductor Multiple-Input Single-Output Boost Converter," in *Proc. IEEE Energy Conversion Congress and Exposition (ECCE)*, 2018.
- [13] H. Tao, J. L. Duarte, and M. A. M. Hendrix, "Multiport Converters for Hybrid Power Sources," *IEEE Power Electronics Specialists Conference*, pp. 3412–3418, 2008.
- [14] H. Matsuo, K. Kobayashi, Y. Sekine, M. Asano, and L. Wenzhang, "Novel solar cell power supply system using the multiple-input DC-DC converter," in *Proc. IEEE Telecommunications Energy Conference (INTELEC'98)*, San Francisco, CA, USA, Nov. 1998, pp. 797–802.
- [15] B. G. Dobbs and P. L. Chapman, "A multiple-input DC-DC converter topology," *IEEE Power Electronics Letters*, vol. 1, no. 1, pp. 6–9, Mar. 2003
- [16] H. Tao, A. Kostopoulos, J. L. Duarte, and M. A. M. Hendrix, "Multi-input bidirectional DC-DC converter combining DC-link and magnetic-coupling for fuel cell systems," in *Proc. IEEE Industry Application Society Conference and Annual Meeting (IAS'05)*, Hong Kong, China, Oct. 2005, pp. 2021–2028.
- [17] L. Solero, A. Lidozzi, and J. A. Pomilio, "Design of multiple- input power converter for hybrid vehicles," in *Proc. IEEE Applied Power Electronics Conference and Exposition (APEC'04)*, Anaheim, California, Feb. 2004, pp. 1145–1151.
- [18] D. Sadeghpour and J. Bauman, "High-Efficiency Coupled-Inductor Switched-Capacitor Boost Converter With Improved Input Current Ripple," *IEEE Transactions on Industrial Electronics*, vol. 69, no. 8, pp. 7940–7951, Aug. 2022.
- [19] C. L. Wey, C. H. Hsu, and G. N. Sung, "A Single-Inductor Programmable-Output DC–DC Converter for Low Power Applications," in *Proc. IEEE IECON*, pp. 316–320, 2013.
- [20] Alexander khusnerov "Transient and Steady-State Analysis of Single Switched Capacitor Converter" ,March 2019, vol.10 ,International Journal of Power Electronics and Drive Systems (IJPEDS), pp:342-350.
- [21] H. Krishnaswami and N. Mohan, "Three-Port Series-Resonant DC–DC Converter to Interface Renewable Energy Sources with Bidirectional Load and Energy Storage Ports," *IEEE Transactions on Power Electronics*, vol. 24, no. 10, pp. 2289–2297, Oct. 2009.
- [22] A. Khaligh and Z. Li, "Battery, Ultracapacitor, Fuel Cell, and Hybrid Energy Storage Systems for Electric, Hybrid Electric, Fuel Cell, and Plug-In Hybrid Electric Vehicles: State of the Art," *IEEE Transactions on Vehicular Technology*, vol. 59, no. 6, pp. 2806–2814, July 2010.
- [23] M. Forouzes, Y. P. Siwakoti, S. A. Gorji, F. Blaabjerg, and B. Lehman, "Step-Up DC–DC Converters: A Comprehensive Review of Voltage-Boosting Techniques, Topologies, and Applications," *IEEE Transactions on Power Electronics*, vol. 32, no. 12, pp. 9143–9178, Dec. 2017.
- [24] J. M. Carrasco et al., "Power-Electronic Systems for the Grid Integration of Renewable Energy Sources: A Survey," *IEEE Transactions on Industrial Electronics*, vol. 53, no. 4, pp. 1002–1016, Aug. 2006.
- [25] B. Wang, L. Xian, X. Zhang, and H. B. Gooi, "A MPC-Based Method for Single-Inductor Multiple-Input Single-Output Boost Converter," in *Proc. IEEE Energy Conversion Congress and Exposition (ECCE)*, 2018.
- [26] M. Azizi, O. Husev, and D. Vinnikov, "Single-Stage Buck–Boost Inverters: A State-of-the-Art Survey," *Energies*, vol. 15, no. 5, pp. 1622, 2022.
- [27] D. Sadeghpour and J. Bauman, "High-Efficiency Coupled-Inductor Switched-Capacitor Boost Converter With Improved Input Current Ripple," *IEEE Transactions on Industrial Electronics*, vol. 69, no. 8, pp. 7940–7951, Aug. 2022.
- [28] P. Mohseni, S. Mohammadsalehian, M. R. Islam, K. M. Muttaqi, and D. Sutanto, "Ultrahigh Voltage Gain DC–DC Boost Converter With ZVS Switching Realization and Coupled Inductor Extendable Voltage Multiplier Cell Techniques," *IEEE Transactions on Industrial Electronics*, vol. 69, no. 1, pp. 323–335, Jan. 2022.
- [29] S. Hasanpour, T. Nouri, and Y. P. Siwakoti, "High Step-Up SEPIC-Based Trans-Inverse DC–DC Converter With Quasi-Resonance Operation for Renewable Energy Applications," *IEEE Transactions on Industrial Electronics*, vol. 70, no. 1, pp. 485–497, 2022.